HHS Public Access

Author manuscript

Nat Mater. Author manuscript; available in PMC 2009 August 01.

Published in final edited form as:

Nat Mater. 2009 February ; 8(2): 151–158. doi:10.1038/nmat2357.

Infection-Mimicking Materials to Program Dendritic Cells In Situ

Omar A. Ali[1], **Nathaniel Huebsch**[1,3], **Lan Cao**[1], **Glenn Dranoff**[4], and **David J. Mooney**[1,2]

[1]School of Engineering and Applied Sciences, Harvard University, Cambridge, MA 02138

[2]Wyss Institute for Biologically Inspired Engineering, Cambridge, MA

[3]Harvard-MIT Division of Health Sciences and Technology, Dana-Farber Cancer Institute and Department of Medicine, Brigham and Women's Hospital and Harvard Medical School, Boston, MA 02115.

[4]Department of Medical Oncology and Cancer Vaccine Center, Dana-Farber Cancer Institute and Department of Medicine, Brigham and Women's Hospital and Harvard Medical School, Boston, MA 02115.

Abstract

Cancer vaccines typically depend on cumbersome and expensive manipulation of cells in the laboratory, and subsequent cell transplantation leads to poor lymph node homing and limited efficacy. We propose that materials mimicking key aspects of bacterial infection may instead be used to directly control immune cell trafficking and activation in the body. It is demonstrated that polymers can be designed to first release a cytokine to recruit and house host dendritic cells (DCs), and subsequently present cancer antigens and danger signals to activate the resident DCs and dramatically enhance their homing to lymph nodes. Specific and protective anti-tumor immunity was generated with these materials, as 90% survival was achieved in animals that otherwise die from cancer within 25 days. These materials show promise as cancer vaccines, and more broadly suggest that polymers may be designed to program and control the trafficking of a variety of cell types in the body.

Ordinarily, the immune response to cancer is limited, so many cell-based vaccination approaches attempt to enhance the response by isolating and activating DCs ex vivo and then introducing these programmed DCs back into the patient1-3. These activated DCs may home to a lymph node, present antigens to naïve T cells, and stimulate and expand specific T-cell populations that elicit anti-tumor responses1-4. While initial results are promising, they require cell isolations and in vitro DC modifications, leading to two patient procedures,

---

Corresponding author: David J. Mooney Harvard School of Engineering and Applied Sciences 29 Oxford St., 319 Pierce Hall Harvard University Cambridge, MA 02138 Tel: 617-384-9624 e-mail: mooneyd@seas.harvard.edu.

Author Contributions

The experiments were designed by O.A., D.J.M., and G.D. and carried out by O.A., N.H., and L.C. The manuscript was written by O.A. and D.J.M. The principal investigator is D.J.M.

Competing Financial Interests

The authors have competing interests as defined by Nature Publishing Group, or other interests that might be perceived to influence the results and discussion reported in this paper.

high cost, and significant regulatory concerns. More importantly, the vast majority (>90%) of transplanted DCs die and few home to the lymph nodes (~0.5-2.0%)1-2,5,6. Additionally, ex vivo DC modifications may be dependent on culture conditions, and be transient, and, thus, lose effectiveness upon *in vivo* transplantation.

These limitations have led to a call1,2 for strategies to quantitatively manipulate, directly in the body, DC recruitment, activation and finally dispersion to the lymph nodes. Immature DCs patrol peripheral tissues, and upon uptake of foreign substances (antigen) they may mature to express on their surface the receptor CCR7 and major histocompatibility complex (MHC)-antigen, to facilitate lymph node homing and subsequent antigen presentation to T-cells, respectively3,7-8,9-11. Key elements of infection that mobilize and activate DCs include inflammatory cytokines, and "danger signals" related specifically to the infectious agent. The cytokine Granulocyte macrophage colony stimulating factor (GM-CSF), has been identified as a potent stimulator of DC recruitment and proliferation12-14. Cytosine-guanosine oligonucleotide (CpG-ODN) sequences are uniquely expressed in bacterial DNA, and are potent danger signals that stimulate mammalian DC activation and DC trafficking15. Repeated, systemic injections of DC-mobilizing cytokines along with bolus injections of CpG-ODN and tumor antigens can promote limited anti-tumor immunity in animal models of cancer16, but single inoculations of tumor antigens, cytokines and danger signals have failed to produce long-term protective immunity1,2.

Past findings suggest that creating an infection-mimicking microenvironment by appropriately presenting exogenous cytokines (e.g., GM-CSF) and danger signals (e.g., CpG-ODN), in concert with cancer antigen may provide an avenue to precisely control the number and timing of DC trafficking and activation, *in situ*. Polymers are routinely modified to provide specific spatiotemporal delivery of drugs to control cell processes4,17-20. To mimic infection and program cells, though, we hypothesized the polymer system must be designed to not only serve as a drug delivery device, but also as a physical, antigen-presenting structure to which the DCs are recruited, and where DCs reside while they are activated. Development of a material system that could by itself serve as an effective cancer vaccine, eliminating the time, expense and regulatory burden inherent to cell therapies could provide a major advance, particularly if it could achieve this effect without the need for multiple, systemic injections and high total drug loading. This possibility was investigated with a material (poly[lactide-co-glycolide]) and bioactive molecules (GM-CSF and CpG-ODN) that have previously undergone significant clinical testing and have excellent safety profiles15, 17-19,21, in order to allow this approach to move quickly to the clinic if proven successful in animal models.

We first developed a quantitative understanding of the ability of GM-CSF to impact DC recruitment, activation and emigration *in vitro* in order to appropriately design a material system for vaccination. GM-CSF enhanced DC recruitment and proliferation in a dose dependent manner (Fig. 1A-B), as expected. However, high concentrations (>100ng/ml) of GM-CSF inhibited DC migration toward a lymph node derived chemoattractant (CCL19) (Fig. 1C). Immunohistochemical staining revealed that the high concentrations of GM-CSF (500 ng/ml) also down-regulated DC expression of the CCL19 receptor CCR7 and MHCII (Fig. 1D). These results suggest sophisticated control over GM-CSF exposure may be

needed to both recruit and program DCs *in vivo*. If GM-CSF alone is to be used for both purposes its local concentration must be designed to decrease over time in order to release DCs that become trapped in the material. Alternatively, provision of a danger signal (e.g., CpG-ODN) in the local environment may possibly release DCs from GM-CSF inhibition once they reside at the infection-mimicking site.

A macroporous poly-lactide-co-glycolide (PLG) matrix was designed to present GM-CSF, danger signals, and cancer antigens in a defined spatiotemporal manner *in vivo*, and serve as a residence for recruited DCs as they are programmed. GM-CSF was encapsulated (54% efficiency) into PLG scaffolds using a high pressure CO_2 foaming process22. These matrices released approximately 60% of their bioactive GM-CSF load within the first 5 days, followed by slow and sustained release of bioactive GM-CSF over the next 10 days (Fig. 2A); this release profile was chosen to allow diffusion of the factor through the surrounding tissue to effectively recruit resident DCs. PLG matrices loaded with 3 μg of GM-CSF were implanted into the subcutaneous pockets of C57BL/6J mice, and histological analysis at day 14 revealed that the total cellular infiltration into scaffolds was significantly enhanced compared to control (no incorporated GM-CSF) (Fig. 2B and S1A). Analysis for DCs specifically (cells positive for cell surface antigens CD11c and CD86) showed that GM-CSF increased not just the total resident cell number, but also the percentage of cells that were DCs (Fig. 2C and S1B). Importantly, the number of DCs residing in the material as a result of GM-CSF delivery was approximately the same as the number of DCs that are commonly programmed and administered by ex vivo protocols ($\sim 10^6$ cells), and enhanced DC numbers were sustained in the material over time (Fig. S1C). As predicted by *in vitro* testing, the effects of GM-CSF on *in vivo* DC recruitment were time and dose-dependent (Fig 2D and S1B-C).

The dose of GM-CSF delivered from the PLG scaffolds was altered to provide distinct *in vivo* concentration profiles in the surrounding tissue, and regulate DC maturation and dispersion of resident DCs (Fig 2E). Implantation of scaffolds with no GM-CSF led to moderate local levels immediately after implantation that subsequently fell to low levels by day 1-2, and then peaked again at day 5, likely due to the inflammatory response to the surgery and implanted PLG (Fig 2E). Delivery of GM-CSF from the PLG scaffolds led to a similar GM-CSF concentration profile over time, but at much higher local concentrations (Fig. 2E). By approximately doubling the initial dose of GM-CSF, the system attained an order of magnitude difference in the peak levels of GM-CSF in vivo, likely due to endogenous GM-CSF production by resident DCs and leukocytes (Fig. S1D-E). The secondary peak for GM-CSF was found at day 5 for the 3000 ng dose, and at day 7 for the 7000 ng dose (Fig. 2E). Regardless of whether 3000 or 7000 ng doses of GM-CSF were utilized, the activation state of DCs peaked when GM-CSF levels began to subside (at days 10 and 28, respectively) (Fig. 2F and S2) and enter into the optimal concentration range for DC programming, as suggested by the in vitro studies.

The ability of the pulse of GM-CSF to recruit and subsequently release a batch of activated DCs to home to the lymph nodes was then tested. Fluorescein isocyanate (FITC) was incorporated into and painted onto PLG scaffolds, as DCs recruited to the scaffold will ingest this label. The label can be later used to identify these cells following their trafficking

to the inguinal lymph nodes23. At day 2, the 3000 ng dose of GM-CSF led to an inhibition of lymph node homing (Fig. 3A and S3), likely due to the high initial levels of GM-CSF that entrap DCs at the scaffold site (Fig. 1D and 2F). However, as GM-CSF levels subsided, a batch of the recruited, FITC-positive DCs were released from the matrices, resulting in a superior and a sustained DC presence in the lymph nodes (Fig. 3A and S3).

As temporally controlling the local GM-CSF concentration allows one to recruit, and disperse a batch of DCs, the utility of these cells as a cancer vaccine was evaluated by immobilizing melanoma tumor lysates (Fig. 3B) into the matrices to load resident DCs with tumor antigens. These PLG cancer vaccines were implanted into C57BL/6J mice, and 14 days later these mice were injected with highly aggressive and metastatic B16-F10 melanoma cells (Fig. S4)23. All mice implanted solely with blank PLG scaffolds had appreciable tumors within 18 days and had to be euthanized by day 23 (Fig. 3C), in accordance with past reports of the aggressiveness of these cells13,16, 24. Delivery of antigen alone from the PLG scaffolds slightly improved the fate of the mice, as some mice in this group survived until day 40 (Fig. 3C). Strikingly, co-delivery of GM-CSF with antigen dramatically decreased tumor formation, and the optimal GM-CSF dose delayed tumor formation by approximately 40 days in 50% of the animals, and cured 23% of animals (Fig. 3C). Moreover, localized tumor antigen presentation in combination with optimal GM-CSF exposure (400ng) increased the average time before tumor formation by 3-fold as compared to antigen alone, and by nearly 2-fold over non-optimal GM-CSF exposure (Fig. S5). Non-optimal GM-CSF doses in immune competent animals and resultant *in vivo* concentrations likely either did not effectively recruit enough DCs (low doses) or prevented sufficient programming and dispersement of resident DCs within an appropriate time frame (high doses) to prevent tumor growth. Analysis of T-cell infiltration into tumor tissue by immunohistochemistry was next performed to determine if programmed DCs were capable of inducing T-cell activation and homing to tumors. Vaccination with antigen alone resulted in CD4(+) T-cell infiltrates (Fig. 5E and S8). Notably, recruiting and programming a batch of DCs in situ with appropriate GM-CSF presentation resulted in a 2-fold increase in CD8(+) cytotoxic T-cell numbers over blank controls. The vaccine's efficacy was attenuated in CD8 and CD4 T-cell knock-out mice (Fig. S6), attesting to the specific role of CD4 and CD8 T-cells in the immune protection.

We then hypothesized that a continuous process of *in situ* DC programming could potentially be achieved by presenting additional cues that released the DCs from GM-CSF inhibition once they reside in the matrices. In particular, the presentation of synthetic CpG-ODN with exogenous GM-CSF was hypothesized to provide a mimic of bacterial infections, in which cells recruited by inflammatory cytokines are stimulated by local toll-like receptor activating "danger signals", such as CpG-ODN present in bacteria15. CpG-ODN was immobilized to the PLG matrices by first condensing nucleotides with polyethylenimine (PEI) to form cationic nanoparticles, as described previously for plasmid DNA25. Following foaming of a combination of CpG-ODN and PLG particles, the CpG-ODN was largely retained in the matrices (>80% over 25 days) (Fig. S7), likely due to electrostatic interactions with the anionic PLG material25-27. The CpG-ODN immobilization allows for host DCs, recruited by GM-CSF, to uptake these nucleotides locally as they reside in the

matrices. Strikingly, this approach resulted in approximately 2.5 and 4.5 fold increases in the numbers of activated DCs (positive for MHCII and CCR7) in the scaffolds, respectively, over GM-CSF or CpG-ODN delivery alone (Fig. 4A). CpG-ODN presentation enhanced DC activation in the presence of inhibitory GM-CSF levels (>40 ng/ml) *in situ*, indicating a more continuous process of DC recruitment and activation. This infection-mimicking system generated the numbers of activated DCs (>10^6) (Fig. 4A) commonly administered in ex vivo protocols2,4,20,. The magnitude of the immune response with this infection-mimic could be appreciated grossly, as the lymph nodes of these animals were markedly enlarged (Fig. 4B). Most importantly, a 6-fold increase in the number of DCs that were first recruited to the matrices and subsequently dispersed to the lymph nodes was achieved with this system (Fig. 4C).

The ability of continuous DC recruitment, and programming to generate an immune response was next tested in the melanoma model. The vaccine provided significant protection, and the level of protection correlated with the CpG dose. Animal survival increased from 23% to 50% and finally 90% at CpG doses of 0 μg, 10μg and 100μg, respectively (Fig 3C and 4D). This material infection-mimic induced equivalent or better immune protection than that obtained with a widely investigated cell-based therapy (Fig. 4D)13. Materials presenting CpG-ODN with lysates alone had only a 20% survival, indicating the benefit of recruiting DCs with GM-CSF (Fig. 4D). The benefit of providing a residence for recruited DCs while they are programmed was demonstrated by the failure of vaccine formulations consisting of bolus injections of tumor lysates, CpG-ODN, with and without 3000ng of GM-CSF (Fig. 4E). Moreover, injecting GM-CSF loaded PLG microspheres to provide sustained GM-CSF delivery without providing a residence for recruited cells, with bolus CpG-ODN and tumor lyate delivery resulted in little immune protection and animals did not survive over 35 days.

To further examine the mechanism of immune protection with this material system, the subsets of DCs and the endogenous production of cytokines by these cells in materials presenting GM-CSF and CpG-ODN alone or together were analyzed, along with the specificity of the immune response. The delivery of GM-CSF alone enhanced the recruitment of CD11c(+)CD11b(+) myeloid DCs (Fig 5B), whereas CpG-ODN delivery alone had little effect on the overall numbers of this subset. CpG-ODN delivery did, though, increase the number of plasmacytoid DCs at the site (Fig 5A), which have been described to predominantly secrete Thelper(Th)-1 cytokines15,26-27,28, especially type1 interferons and interleukin(IL)-12 that can promote CD8(+), cytotoxic T cell immunity in response to CpG-ODN presentation with antigen18,26,28. Accordingly, CpG signaling not only up-regulated the expression of activation markers on resident DCs (Fig. 4A), but also induced IFN-γ and IL-12 production (Fig. 5C-D) at the vaccine site, as expected from the increased presence of plasmacytoid DCs18,27. Moreover, analysis of T cell infiltrates into tumors that formed in the subset of animals that were not completely protected (infection mimics; 10 μg CpG-ODN dose) revealed that, even in these animals, DC programming with CpG-ODN resulted in an almost 3-fold increase in CD8(+) T-cell infiltration over controls (Fig 5E and S8). Further, tyrosinase-related protein (TRP)-2 is a main antigenic target of the immune response elicited by melanoma vaccines in both mice (including B16 whole cell vaccines)

and humans16,29, and staining cells isolated from spleens with MHC class I/TRP2 peptide pentamers revealed a dramatic expansion of TRP2-specific CD8 T cells in vaccinated mice (Fig. 5F). These antigen-specific T cells are likely involved in the killing of tumor cells, and facilitated immune protection after vaccination. Additionally, 33% of surviving mice developed patches of skin and hair depigmentation starting at the sites of tumor inoculation (back of neck) (Fig S9). Depigmentation, which likely involves T cell responses to melanocyte antigens30, has been correlated to improved clinical responses in human melanoma patients31,32, and, in these studies, was only observed in mice treated with infection mimics.

These results indicate that appropriately mimicking aspects of infection with material systems can dramatically impact tumor progression by effectively recruiting, activating and homing DCs to lymph nodes. The first approach utilized a pulse of GM-CSF alone to recruit DCs to the tumor-antigen presenting material. The DCs subsequently resided within the material and were trapped until GM-CSF levels fell and cells could become activated and disperse. These finding are consistent with previous reports using sustained GM-CSF delivery at vaccine sites13,16, but further indicate the specific concentration and duration of GM-CSF are critical to its effects. A continuous process was subsequently developed to shuttle DCs through an infectious-like microenvironment via recruitment with GM-CSF, followed by activation of resident DCs via CpG-ODN presentation, and subsequent release. The presentation of PEI condensed CpG-ODN from the material dramatically increased not only the numbers of activated, host DCs residing in the material, but also the percentage and total numbers of programmed DCs that emigrated to the lymph nodes. Further, CpG-ODN signaling selected for specific DC subsets and DC functions associated with protective immune responses. These models may in the future be useful to study DC responses to various other stimuli (antigenic and danger) in vivo, and as control systems for antigen-specific immune activation.

The system’s quantitative control over DC trafficking and activation translated to a regulation over the efficacy of the cancer vaccine. As the numbers of DCs that were programmed and dispersed to the lymph nodes increased, the survival increased from 0 to 25 and finally 90%. T-cells mediated immune protection, as a clear relation between the numbers of T cells in the tumors that did form (Figs. 5E) and vaccine efficacy was found, and infection mimics induced the generation of melanoma-antigen specific T cells. The matrix structure was necessary to produce long-lasting immunity, as vaccines delivered in bolus form and sustained release without provision of a cell residence failed to produce significant protective immunity. Although previous reports concluded that either cell transplantation or multiple systemic injections are necessary to promote protective immunity in clinically relevant tumor models16, 29-31, we demonstrate here that appropriately designed materials can provide significant and specific immune protection that is equal to or superior to previous reports, even with single application at vastly reduced total drug doses (e.g., 3 μg in the scaffold system vs. 100’s μg total dose in repeated, systemic injections)16,33. The tumor lysate utilized in this report contain a mixture of tumor associated proteins, which may dilute the material’s presentation of strong rejection antigens

(e.g. Trp2 in melanoma), to DCs *in situ*, and it may be advantageous to use purified antigens in future vaccine protocols.

These current findings have significant clinical relevance, as the material system programmed DCs *in situ*, and not only bypassed the complication and cost of ex vivo cell manipulation and transplantation, but also provided tight control over the number of DCs recruited, activated and dispersed to the lymph nodes. Although the implantable nature of this system is not ideal, cancer patients routinely undergo invasive and destructive procedures in an effort to cure their disease. Indeed, patients accept implantable systems (e.g. Implanon)34, even in non life-threatening situations. This material approach may provide an alternative to current cancer vaccines, or could also be used in concert with those and other approaches.

More broadly, this study demonstrated a powerful new application for polymeric biomaterials that may potentially be utilized to treat a variety of diseases by programming or reprogramming host cells in situ. This system may be applicable to other situations in which one desires to promote a destructive immune response (e.g., eradicate infectious diseases) or to promote tolerance (e.g., subvert autoimmune disease). Further, the general concept of using polymers as a temporary residence for *in situ* cell programming may provide a new approach to using polymers therapeutically, and a powerful alternative to current cell therapies that depend on ex vivo cell manipulation (e.g., stem cell therapies).

Methods

Matrix Fabrication

A 85:15, 120 kD copolymer of D,L-lactide and glycolide (PLG) (Alkermes, Cambridge, MA) was utilized in a gas-foaming process to form macroporous PLG matrices22. PLG microspheres encapsulating GM-CSF were made using standard double emulsion35. To incorporate tumor lysates, biopsies of B16-F10 tumors that had grown subcutaneously in the backs of C57BL/6J mice (Jackson Laboratory, Bar Harbor Maine), were digested in collagenase (250 U/ml) (Worthington, Lakewood, NJ), and subjected to 4 cycles of rapid freeze in liquid nitrogen and thaw (37°C) and then centrifuged at 400 rpm for 10 min. The supernatant containing tumor lysates was collected and lyophilized with the PLG microspheres and the resulting mixture was used to make PLG scaffold-based cancer vaccines. To incorporate CpG-ODNs into PLG scaffolds, CpG-ODN 1826, 5'-tcc atg acg ttc ctg acg tt-3', (Invivogen, San Diego, CA) was first condensed with poly(ethylenimine) (PEI, *M*w ∼25,000 g mol—1, Sigma Aldrich) molecules by dropping ODN-1826 solutions into PEI solution, while vortexing the mixture25. The charge ratio between PEI and CpG-ODN (NH3+:PO4-) was kept constant at 7 during condensation. PEI-CpG-ODN condensate solutions were then vortexed with 60 μl of 50% (wt/vol) sucrose solution, lyophilized and mixed with dry sucrose to a final weight of 150 mg. The sucrose containing condensates was then mixed with blank, GM-CSF and/or tumor lysate loaded PLG microspheres to make PLG cancer vaccines.

To determine the efficiency of GM-CSF incorporation and the kinetics of GM-CSF release from PLG scaffolds, ^{125}I-labeled hr-GM-CSF (Perkin Elmer) was utilized as a tracer, and

standard release studies were performed (details provided in supplemental materials). Similarly, the amount of melanoma protein incorporated into scaffolds and released into PBS media was assessed by a protein assay (BioRad Laboratories, Hercules, CA). The amount of CpG-ODN incorporated into PLG scaffolds and released into PBS was determine by absorbance readings (260/280 and 260/230 ratios calculated at 0.2 mm pathlength) using a Nanodrop instrument, ND1000 (Nanodrop technologies, Wilmington, DE). To determine GM-CSF concentrations at the scaffold implant site, adjacent tissue was excised and digested with tissue protein extraction reagent (Pierce). The GM-CSF concentration in the tissue was then analyzed with ELISA (R&D systems), according to the manufacturer's instructions.

In vivo DC migration and activation assays

Blank scaffolds and scaffolds containing GM-CSF with or without 10 μg PEI-ODN control (5'- tcc atg agc ttc ctg agc tt -3') or 10 μg PEI-CpG-ODN condensate loaded scaffolds were implanted into subcutaneous pockets on the back of 7-9 week old male C57BL/6J mice. For histological examination scaffolds were excised, paraffin-embedded, and stained with hematoxylin and eosin. To analyze DC recruitment isolated cells were counted using a Z2 coulter counter (Beckman Coulter), and subsets of the total cell population were then stained with primary antibodies (BD Pharmingen, San Diego, CA) conjugated to fluorescent markers to allow for analysis by flow cytometry. To track DC emigration from the implant site FITC was incorporated into the scaffolds22.

Tumor growth assays, and T cell responses

PLG scaffolds with melanoma tumor lysates and various dosages of GM-CSF and/or various quantities PEI-CpG-ODN condensates were implanted subcutaneously into the lower left flank of C57BL/6J mice. Animals were challenged 14 days later with a subcutaneous injection of 10^5 B16-F10 melanoma cells (ATCC, Manassas, NJ) in the back of the neck. Animals were monitored for the onset of tumor growth (approximately $1mm^3$) and sacrificed for humane reasons when tumors grew to 20 - 25 mm (longest diameter). For histological examination, tumors were biopsied at days 20-25 after injection and fixed in Z-fix (Anatech, Battle Creek, MI) and paraffin-embedded. To examine tumor tissue for T-cell infiltration, immunoperoxidase staining was performed using the avidin-biotinperoxidase Vectastain Elite ABC kit (Vector Laboratories). To determine the IL-12 and IFN-γ concentration at the matrix implant site, adjacent tissue was excised and digested with tissue protein extraction reagent (Pierce). The IL-12 and IFN concentration in the tissue was then analyzed with ELISA (R&D systems), according to the manufacturer's instructions.

To determine the generation of TRP-2-specific, cytotoxic T lymphocytes, single cell suspensions were prepared from the spleens of both naïve mice and mice immunized with PLG infection mimics (Antigen+3000ng GM-CSF+ 10μg CpG) for 30 days. These cells were initially stained with APC-H-2Kb/TRP2 pentamers (Proimmune,, Oxford Science Park, UK), and subsequently stained with PE-anti-CD8 mAb (mAb (BD Pharmingen, San Diego).

PLG cancer vaccines were compared to a common cell-based vaccine using B16-F10 melanoma cells that were genetically modified to express GM-CSF, and subsequently irradiated (3500rad), as described previously16. The irradiated tumor cells (5×10^5 cells) were then injected subcutaneously into C57BL/6J mice that were challenged 14 days later with 10^5 B16-F10 melanoma cells.

Supplementary Material

Refer to Web version on PubMed Central for supplementary material.

Acknowledgements

We are grateful to the Bauer research centers at Harvard University for assistance in NanoDrop measurements of nucleotide content. We thank B. Tilton for technical assistance with flow cytometry. The project has been made possible by NIH funding (NIH R01 DE013033) and internal funding at Harvard University to D.J.M.

References

1. Banchereau J, Steinman RM. Taking dendritic cells into medicine. Nature. 2007; 49:419–426. [PubMed: 17898760]
2. Gilboa E. Dendritic cell based vaccines. J Clin Invest. 2007; 117:1195–1203. [PubMed: 17476349]
3. Banchereau J, Steinman RM. Dendritic cells and the control of immunity. Nature. 1998; 392
4. Schuler G, Schuler-Thurner B, Steinman RM. The use of dendritic cells in cancer immunotherapy. Curr Opin Immunol. 2003; 15:138–147. [PubMed: 12633662]
5. U.S. National Institutes of Health. 2007http://clinicaltrials.gov
6. Kleindienst P, Brocker T. Endogenous dendritic cells are required for amplification of T cell responses induced by dendritc cell vaccine in vivo. J. Immunol. 2003; 170:2817–2823. [PubMed: 12626531]
7. Celluzzi CM, Mayordomo JI, Storkus WJ, Lotze MT, Falo LD Jr. Peptide- pulsed dendritic cells induce antigen-specific, CTL-mediated protective tumor immunity. J. Exp. Med. 1996; 183:283–287. [PubMed: 8551233]
8. Jenne L, Arrighi JF, Jonuleit H, Saurat JH, Hauser C. Dendritic cells containing apoptotic melanoma cells prime human CD8+ T cells for efficient tumor cell lysis. Cancer Res. 2000; 60:4446–4452. [PubMed: 10969791]
9. Mellman I, Steinman RM. Dendritic cells: specialized and regulated antigen processing machines. Cell. 2001; 106(3):255–8. [PubMed: 11509172]
10. Sozzani S, et al. Differential regulation of chemokine receptors during Dendritic cell maturation: a model for their trafficking properties. J. Immunol. 1998; 161:1083–1086. [PubMed: 9686565]
11. Yanagihara S, Komura E, Nagafune J, Watari H, Yamaguchi Y. EB1/CCR7 is a new member of dendritic cell chemokine receptor that is upregulated upon maturation. J. Immunol. 1998; 161:3096–3102. [PubMed: 9743376]
12. Dieu MC, et al. Selective recruitment of immature and mature dendritic cells by distinct chemokines expressed in different anatomic sites. J. Exp. Med. 1988; 188:373–386. [PubMed: 9670049]
13. Dranoff G, et al. Vaccination with irradiated tumor cells engineered to secrete murine granulocyte macrophage colony-stimulating factor stimulates potent, specific, and long-lasting anti-tumor immunity. Proc. Natl. Acad. Sci. USA. 1993; 90:3539–3543. [PubMed: 8097319]
14. Randolph GJ, Ochando J, Partida-Sanchez S. Migration of dendritic cell subsets and their precursors. Annu. Rev. Immunol. 2008; 26:293–316. [PubMed: 18045026]
15. Klinman DM. Immunotherapuetic uses of CpG oligodeoxynucleotides. Nat. Rev. Immunol. 2004; 4:249–58. [PubMed: 15057783]

16. Okano F, Merad M, Furumoto K, Engleman EG. In vivo manipulation of dendritic cells overcomes tolerance to unmodified tumor-associated self antigens and induces potent antitumor immunity. J Immunol. 2005; 174(5):2645–52. [PubMed: 15728471]
17. Sheridan MH, Shea LD, Peters MC, Mooney DJ. Bioabsorbable polymer scaffolds for tissue engineering capable of sustained growth factor delivery. J. Control Release. 2000; 64(1-3):91–102. [PubMed: 10640648]
18. Richardson TP, Peters MC, Ennett AB, Mooney DJ. Polymeric system for dual growth factor delivery. Nature Biotech. 2001:1029–1034.
19. Griffith LG. Emerging design principles in biomaterials and scaffolds for tissue engineering. Ann N Y Acad Sci. 2002; 961:83–95. [PubMed: 12081872]
20. Ali, OA.; Mooney, DJ. Cell Transplantation from Laboratory to Clinic. Elsevier Inc; Burlington, MA: 2006. “Converging Cell Therapy with Biomaterials.”; p. 591-609.
21. Disis ML. Clinical use of subcutaneous G-CSF or GM-CSF in malignancy. Oncology. 2005; 19(4): 5–9. [PubMed: 15934493]
22. Harris LD, Kim BS, Mooney DJ. Open pore biodegradable matrices formed with gas foaming. J. Biomed.Mater. Res. 1998; 42:396–402. [PubMed: 9788501]
23. Thomas WR, Edwards AJ, Watkins MC, Asherson GL. Distribution of immunogenic cells after painting with the contact sensitizers fluorescein isothiocyanate and oxazolone. Different sensitizers form immunogenic complexes with different cell populations. Immunobiology. 1980; 39:21–27.
24. Fidler IJ. Biological behavior of melanoma cells correlated to their survivial in vivo. Cancer Research. 1975; 35:218–234. [PubMed: 1109790]
25. Huang YC, Connell M 1, Park Y, Mooney DJ, Rice KG. Fabrication and in vitro testing of polymeric delivery system for condensed DNA. J Biomed. Mater. Res. 2003; 67:1384–1392.
26. Krieg AM. Development of TLR9 agonists for cancer therapy. J Clin Invest. 2007; 17:1184–94. [PubMed: 17476348]
27. Kanzler H, Barrat FJ, Hessel EM, Coffman RL. Therapeutic targeting of innate immunity with Toll-like receptor agonists and antagonists. Nat. Med. 2007; 13:552–559. [PubMed: 17479101]
28. Kapsenberg M. Dendritic-cell control of pathogen-driven T-cell polarization. Nat Rev Immunol. 2003; 12:984–93. [PubMed: 14647480]
29. De Palma R, et al. Therapeutic Effectiveness of Recombinant Cancer Vaccines Is Associated with a Prevalent T-Cell Receptor Usage by Melanoma-specific CD8 T Lymphocytes. Can Res. 2004:8068–8076.
30. Okamoto T, et al. Anti-tyrosinase-related protein-2 immune response in vitiligo patients and melanomapatients receiving active-specific immunotherapy. J. Invest. Dermatol. 1998; 111:1034–1039. [PubMed: 9856813]
31. Richards JM, Mehta N, Ramming K, Skosey P. Sequential chemoimmunotherapy in the treatment of metastatic melanoma. J. Clin. Oncol. 1992; 10:1338–1343. [PubMed: 1634924]
32. Rosenberg SA, White DE. Vitiligo in patients with melanoma: normal tissue antigens can be targets for cancer immunotherapy. J. Immunother. Emphasis Tumor Immunol. 1996; 19:81–84. [PubMed: 8859727]
33. Overwijk WW, et al. Autoimmunity after reversal of a functionally tolerant state of self-reactive CD8+ T cells. J Exp Med. 2003; 4:569–80. [PubMed: 12925674]
34. Fischer MA. Implanon: a new contraceptive implant. J Obstet Gynecol Neonatal Nurs. 2008; 37(3):361–8.
35. Cohen S, Yoshioka T, Lucarelli M, Hwang LH, Langer R. Controlled delivery systems for proteins based on poly(lactic/glycolic acid) microspheres. Pharm. Res. 1991; 8:713–720. [PubMed: 2062800]

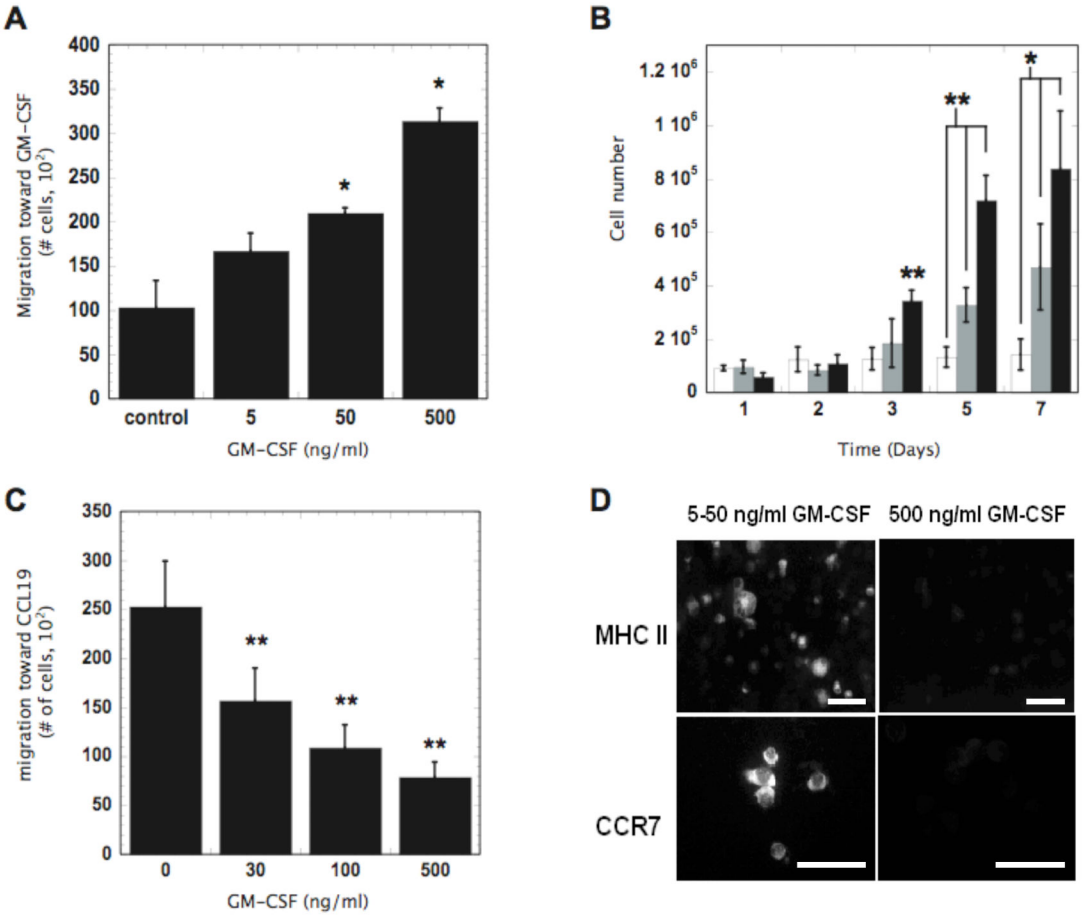

Figure 1. The concentration dependent effects of GM-CSF on DC proliferation, recruitment, activation and emigration in vitro: implications for in situ programming systems

(A) The in vitro migration of JAWSII DCs induced by the indicated concentrations of GM-CSF in transwell systems. Migration counts measured at 12 hours. (B) The effects of GM-CSF concentration on the proliferation of JAWSII DCs. 0 (□), 50 (■), and 500 ng/ml (■) of GM-CSF. (C) The effects of the indicated concentrations of GM-CSF on JAWS II DC emigration from the top wells of transwell systems toward media supplemented with 300 ng/ml CCL19. Migration counts taken at 6 hours. (D) Representative photomicrographs of TNF-α and LPS stimulated JAWSII DCs cultured in 5-50 or 500 ng/ml GM-CSF and stained for the activation markers MHCII and CCR7. Scale bar in (D) - 20 μm. Values in (A-C) represent mean and standard deviation (n=4) and * $P<0.05$ ** $P<0.01$

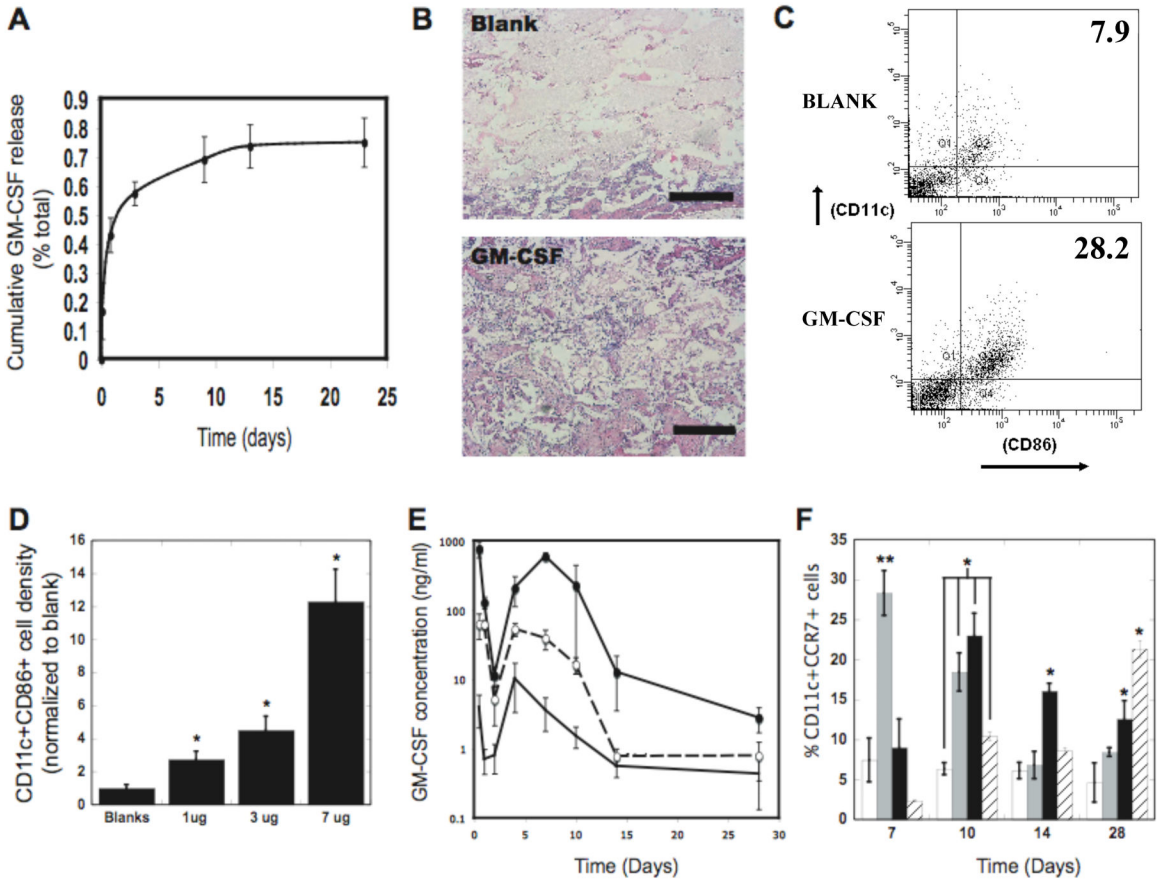

Figure 2. In vivo control of DC recruitment and programming

(A) Cumulative release of GM-CSF from PLG matrices over a period of 23 days. (B) H&E staining of sectioned PLG scaffolds explanted from subcutaneous pockets in the backs of C57BL/6J mice after 14 days: Blank scaffolds, and GM-CSF (3000 ng) loaded scaffolds. (C) FACS plots of cells isolated from explanted scaffolds and stained for the DC markers, CD11c and CD86. Cells were isolated from blank and GM-CSF (3000 ng) loaded scaffolds implanted for 28 days. Numbers in FACS plots indicate the percentage of the cell population positive for both markers. D) The fractional increase in CD11c(+)CD86(+) DCs isolated from PLG scaffolds at day 14 after implantation in response to doses of 1000, 3000 and 7000ng of GM-CSF, as normalized to the blank control (Blanks). (E) The in vivo concentration profiles of GM-CSF at the implant site of PLG scaffolds incorporating 0 (-), 3000 (--○--), and 7000 ng (--●--) of GM-CSF as a function of time post implantation. (F) The percentage of CD11c(+)CCR7(+) host DCs isolated from scaffolds loaded with 0 (□), 400 (■), 3000ng (■), and 7000 ng of GM-CSF (▩) as a function of time after implantation into the backs of C57BL/6J mice. Scale bar in B — 500 μm. Values in A, D, E, and F represent mean and standard deviation (n=4 or 5). * $P<0.05$ ** $P<0.01$.

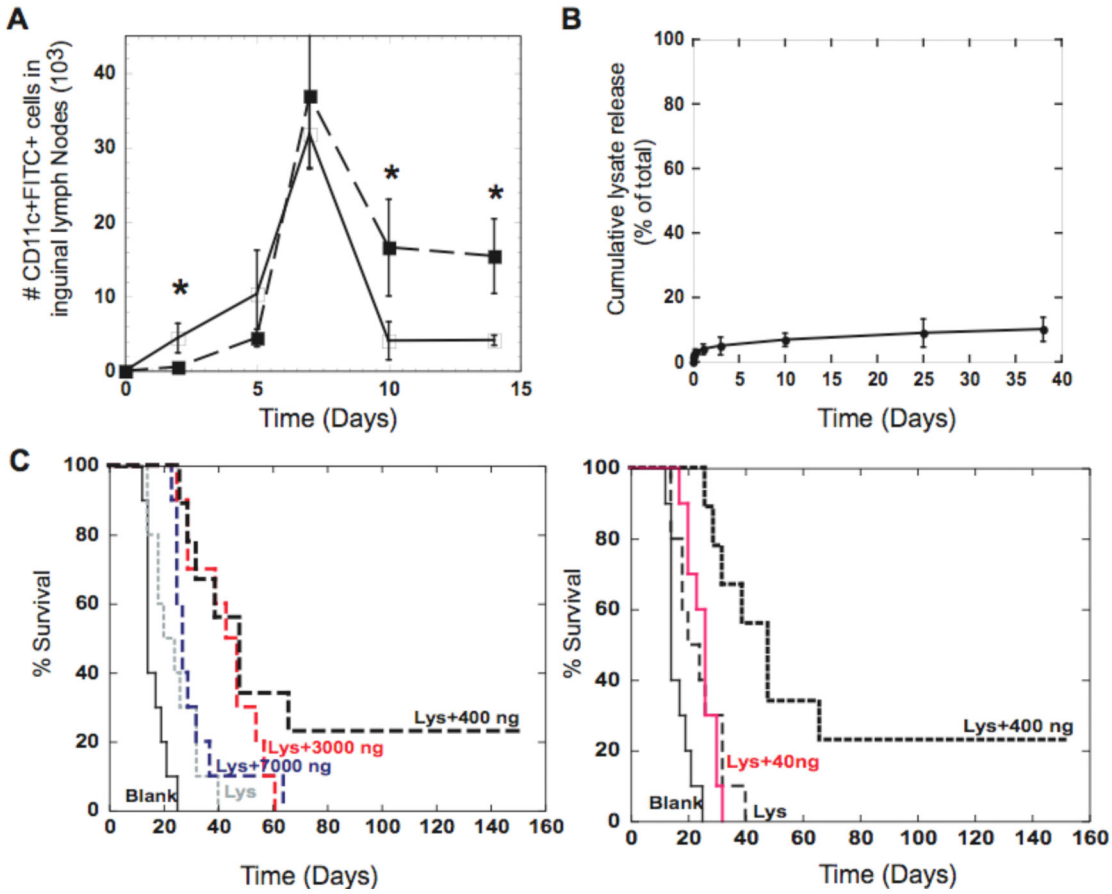

Figure 3. Batches of DCs programmed in situ infer anti-tumor immunity

(A) The number of FITC(+) DCs that had homed to the inguinal lymph nodes as a function of time subsequent to their residence at FITC painted blank scaffolds (-□-) and FITC painted GM-CSF loaded (3000 ng) scaffolds (-■-). (B) Cumulative release of tumor lysates (--■--) delivered from PLG Scaffolds (85:15, 120kD) demonstrates that tumor antigens are immobilized within the scaffold. (C) The survival time after PLG cancer vaccines were implanted into mice to appropriately expose host DCs to B16-F10 tumor lysates and 40, 400, 3000, and 7000 ng of GM-CSF. At Day 14 after vaccination, C57BL/6J mice were challenged with 10^5 B16-F10 melanoma tumor cells and monitored for animal survival. Day 0 on survival curves represents the day of tumor challenge. Values represent the mean and standard deviation (A, B; n=4 or 5) (C; n=9 or 10). * $P<0.05$** $P<0.01$.

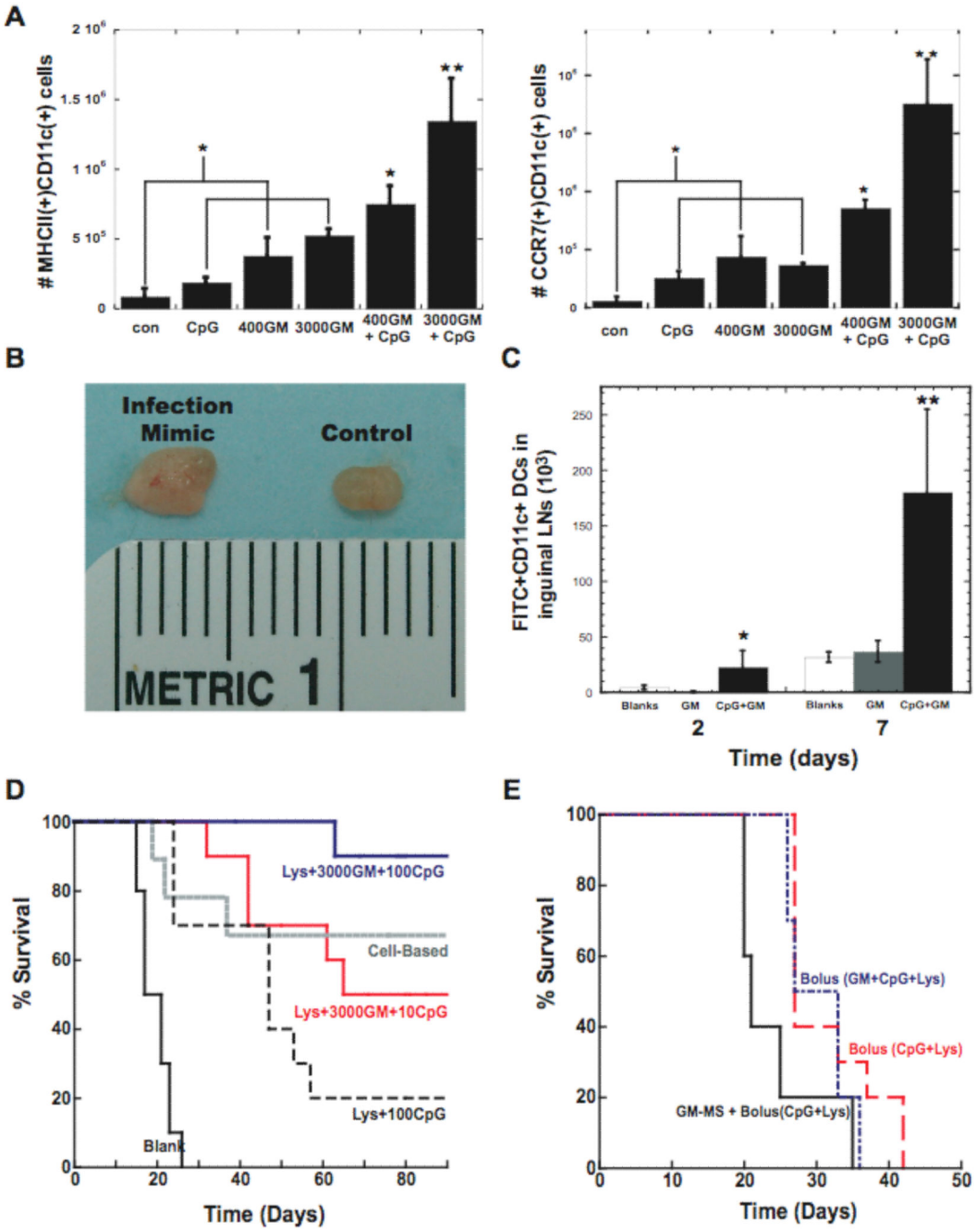

Figure 4. Infection-mimicking microenvironment confers potent anti-tumor immunity

(A) The number of CD11c(+)MHCII(+) and CD11c(+)CCR7(+) host DCs isolated from matrices loaded with PEI-ODN control, 10 μg PEI-CpG-ODN, 400 and 3000ng GM-CSF, and 400 and 3000ng GM-CSF in combination with 10 μg PEI-CpG-ODN at Day 7 after implantation. (B) Digital photograph of inguinal lymph nodes from normal mice (control) and after 10 days implantation of matrices incorporating 10 μg CpG-ODN + 3000ng GM-CSF (infection-mimic). (C) The number of FITC(+)CD11c(+) DCs present in the inguinal lymph nodes at 2 and 7 days after implantation of FITC painted matrices [control (Blanks),

GM-CSF loaded matrices (GM), GM-CSF and CpG-ODN matrices(CpG-GM)]. (D) A comparison of the survival time in mice treated with blank PLG scaffolds, antigen+100μg CpG-ODN (Lys+100CpG), antigen+3000ng GM-CSF+10μg CpG-ODN (Lys+3000GM +10CpG), and antigen+3000ng GM-CSF+ 100μg CpG-ODN (Lys+3000GM+100CpG). Animals were also immunized using a cell-based vaccine (cell-based). (E) The survival time of mice vaccinated with bolus injections of CpG-ODN+antigen (Bolus(CpG+Lys)), bolus injections of CpG-ODN, antigen, and GM-CSF (Bolus(GM+CpG+Lys)) or with PLG microspheres releasing GM-CSF combined with injection of CpG-ODN and antigen [GM-CSF+Bolus(CpG+Lys)]. Mice were challenged (Day 0 on graphs) with 10^5 B16-F10 melanoma tumor cells and monitored for the onset of tumor occurrence. GM-CSF dose was 3000ng and CpG-ODN dose was 10μg. Values represent the mean and standard deviation (A, C; n=3 or 4) (D,E; n=9 or 10). * $P<0.05$** $P<0.01$.

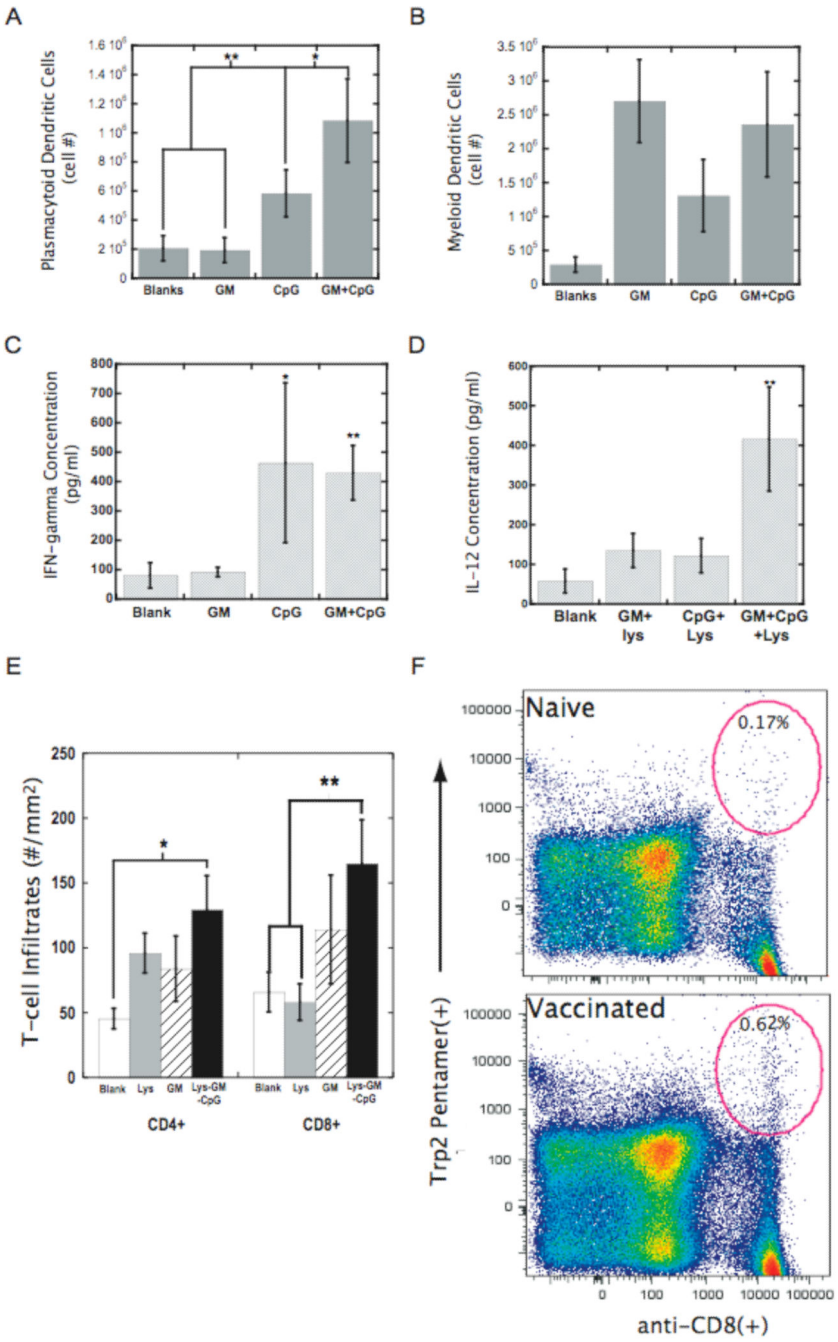

Figure 5. Infection mimics amplify TH1 induction and promote antigen specification during immune responses

The number of plasmacytoid DCs (CD11c+PDCA-1+) (A) and myeloid DCs (CD11c +CD11b+) (B) isolated from blank matrices (Blanks) or matrices loaded with either 3000ng of GM-CSF (GM) or 100 μg PEI-CpG-ODN (CpG) or the combination of GM-CSF and PEI-CpG-ODN (GM+CpG) at Day 7 after implantation. The in vivo concentrations of (C) IFN-γ and (D) IL-12 at the implant site of blank matrices (Blanks) or matrices loaded with either 3000ng of GM-CSF (GM) or 100 μg PEI-CpG-ODN (CpG) or the combination of GM-CSF and PEI-CpG-ODN (GM+CpG) at Day 7 after implantation into the backs of

C57BL/6J mice. For IL-12 analysis all conditions also contained antigen (+Lys). (E) T cell infiltrates into tumors of animals treated with blank PLG scaffolds (□), PLG scaffolds incorporating tumor lysates (Lys), lysates+3000ng GM-CSF (GM), or lysates+3000ng GM-CSF+10 μg CpG-ODN (Lys+GM+CpG). (F) Splenocytes from naïve mice (naïve) and mice treated with PLG vaccines (vaccinated) were stained with anti-CD8-FITC Ab, anti-TCR -APC Ab, and Kb/TRP2 pentamers. The ellipitical gates in the upper right quadrant represent the TRP2-specific, CD8(+) T cells and numbers provide percentage of positive cells. Values in A-E represent the mean and standard deviation (n=4 or 5). * $P<0.05$** $P<0.01$.